Environ Earth Sci (2012) 65:741–752
DOI 10.1007/s12665-011-1120-y

ORIGINAL ARTICLE

Hydrogeochemical study of the thermal and mineralized waters of the Banaz (Hamamboğazi) area, western Anatolia, Turkey

Suzan Pasvanoğlu

Received: 6 October 2010 / Accepted: 13 May 2011 / Published online: 3 June 2011

Abstract The Hamamboğazi spa in western Turkey was built around natural hot springs with discharge temperatures in the range of 30–54°C; the waters have near neutral pH values of 6.50–7.10 and a TDS content between 2,694 and 2,982 mg/l. Thermal water with a temperature of 47.5–73°C has been produced at 325 l/s from five wells since 1994, causing some springs to go dry. A management plan is required in the study area to maximize the benefits of this resource, for which currently proposed direct uses include heating in the district and greenhouses, as well as balneology in new spas in the area. The best use for the water from each spring or well will depend on its temperature, chemistry and location. The thermal waters are mixed Na–Mg–HCO_3–SO_4 fluids that contain a significant amount of CO_2 gas. The chemical geothermometers applied to the Hamamboğazi thermal waters yield a maximum reservoir temperature of 130°C. Isotope results (^{18}O, ^{2}H, ^{3}H) indicate that the thermal waters have a meteoric origin: rainwater percolates downward along fractures and faults, is heated at depth, and then rises to the surface along fractures and faults that act as a hydrothermal conduit. The basement around the Banaz Hamamboğazi resort is comprised of Paleozoic metamorphic schist and marbles exposed 8 km south and 15 km north of Banaz. Mesozoic marble, limestone and ophiolitic complex are observed a few km west and in the northern part of Banaz. These units were cut at a depth of 350–480 m in boreholes drilled in the area. Overlying lacustrine deposits are composed of fine clastic units that alternate with gypsum, tuff and tuffites of 200–350 m thickness. The marble and limestones form the thermal water aquifer, while lacustrine deposits form the impermeable cap.

Keywords Hamamboğazi thermal spring · Hydrogeochemistry · Stable isotope · Banaz · Turkey

S. Pasvanoğlu (✉)
Faculty of Engineering, Geological Engineering Department, University of Kocaeli, Izmit, Kocaeli, Turkey
e-mail: suzan@kocaeli.edu.tr

Introduction

The geothermal fields of western Turkey provide a unique setting of high enthalpy combined with a large variation in the chemical compositions of geothermal fluids. The distribution of the thermal systems follows the tectonic patterns of Turkey. The presence of active structural systems that characterize western Anatolia is associated with young acidic volcanic activity, grabens, hydrothermal alteration, fumarols and thermal springs (Canik and Başkan 1983; Ercan 1982; Ercan et al. 1997; Şimşek 1997).

The Uşak-Banaz region in western Anatolia comprises an area of about 20 km^2 (Fig. 1). The Hamamboğazi spa is located on the eastern flank of the Hamamboğazi valley 7 km NE of the town of Banaz at an elevation of 970 m. This area is covered by the 1:25,000 scale Uşak-K23-b4 quadrangle map. Thermal waters of the Hamamboğazi spa are manifested through NE-SW trending normal faults. Their temperature and discharge are in the range of 30–54°C and 0.67–45 l/s, respectively. During recent years, there has been rather limited geothermal research activity in the area, even though exploitation has increased considerably. Exploration in the Banaz Hamamboğazi area was started in 1994 by the General Directorate of Mineral Research and Exploration of Turkey (MTA). As a result of drilling to a depth of 245–480 m, thermal water with a temperature of 62–73°C has been produced at a flowrate of 125 l/s (Pasvanoglu et al. 2005) from four wells since

1994. In addition, a new well was completed in 2010 by the General Directorate of Provincial Banks (ILB), reaching a depth of 207 m and temperature of 47.5°C. The flowrate of the thermal water is 200 l/s (Öngür 2010b).

The area is a tourist attraction because of its thermal waters, which are used for agriculture and bathing purposes. Detailed geological, geochemical and isotopic investigations on the thermal springs have been carried out

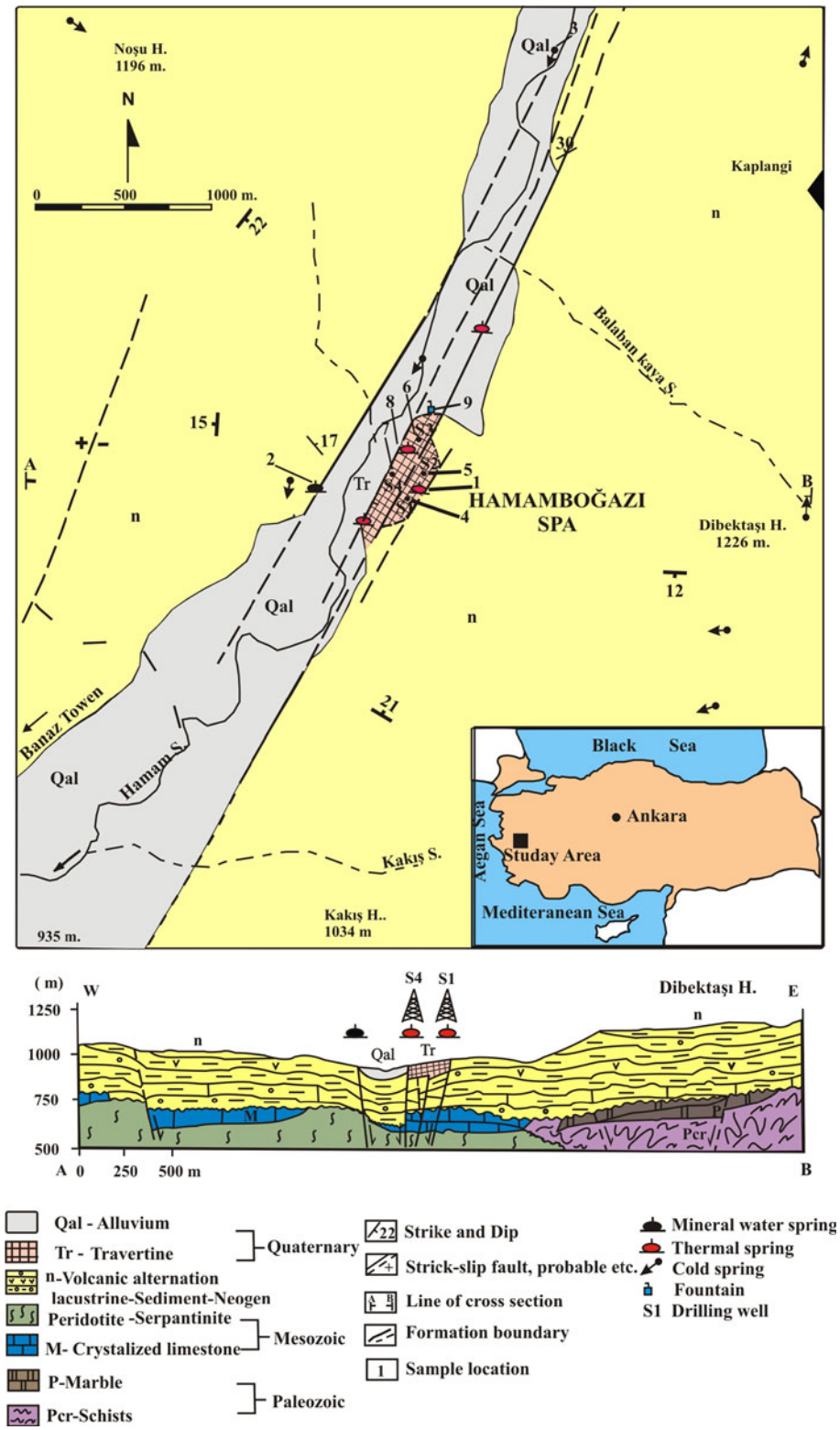

Fig. 1 Geological map and cross section of the study area

in order to understand their chemical evolution and estimate the reservoir temperatures using chemical geothermometers. Results of various geothermometers were evaluated to assess potential geothermal energy use. Application for heating in the district and greenhouse heating as well as the concept of creating new spas in the area are being seriously considered by the Banaz Municipality.

Materials and methods

The study was conducted in three stages as (1) field observations, (2) sampling, and (3) data processing and interpretation of the results. During the field work, a geological map of the hot springs area was completed at 1:25,000 scale (Fig. 1). In order to determine hydrochemical and isotopic compositions of thermal waters, thermal and cold waters were sampled in July 2003 (Table 1). Samples were collected from the thermal spring and wells that are used in Banaz spa and from cold waters representing the groundwater in the area. Locations of the water samples are shown in Figs. 1 and 2. All water samples were collected into high-density polyethylene containers, and 0.2 ml concentrated HNO_3 was added to 100-ml samples for cation and trace element analyses. The other batch (1,000 ml) taken for anion analyses was untreated. Samples of 100 and 200 ml volume were collected for $\delta^{18}O$–δD and $\delta^{3}H$ analyses, respectively. Chemical, heavy metal and isotope analyses were conducted at the State Hydraulic Works (DSI) Laboratory of Turkey, Ankara. Titration methods were used for alkalinity (HCO_3) and Cl analyses. SO_4 and SiO_2 concentrations were determined by spectrophotometry. The temperature of the waters, the pH and electrical conductivity (EC) measurements were carried out both at the sampling sites and in the laboratory. The results for pH showed differences of approximately one unit ($pH_{lab} > pH_{field}$), presumably because of degassing of CO_2. Water chemistry analyses were conducted in accordance with APHA (1989), AWWA and WPCF international standards. The charge balance of the thermal waters is generally less than 6%. Accuracy of isotope analyses is 0.15‰ for $\delta^{18}O$ and 2‰ for δD. In addition, results of previous analyses were also utilized for the evaluation of water chemistry data.

Geology

Paleozoic, Mesozoic and Tertiary rocks are exposed around the Banaz area (Figs. 1, 2). The basement is represented by metamorphic rocks that are a northeastern elongation of the Menderes massif exposed 8 km south of Banaz and the southern flank of Murat Mountain (15 km north of Banaz). Metamorphic rocks generally develop in green schist facies and are overlain by Upper Paleozoic-Lower Mesozoic marbles. Schist and marbles continue with an ultrabasic complex series of Upper Mesozoic age exposed 4 km west and northwest of Banaz. This sequence consists of various limestones, radiolarites, cherts, serpentinites and peridotites. Older formations are overlain by Neogene lacustrine deposits widely exposed around the Banaz area. Except for alluvial deposits filling the Hamam stream valley around the spa, lacustrine deposits are observed throughout the study area. Lacustrine units are composed of conglomerates, sandstone, limestone, siltstone, claystone, marl and their alternations. Tuff and tuffire bands as well as gypsum levels are also detected in between. In wells drilled around the Hamamboğazi spa, their thickness was found to be more than 300 m. They exhibit well bedding. Layers have various dips and strikes, generally between 12 and 30 (Pasvanoğlu et al. 2005). Trace fossils are observed in fine-grained sandstones around the Kaplangi village. Alluvial deposits filling the Hamam stream valley have a thickness of 20–25 m. In areas where rivers join with valleys, alluvium is mixed with talus and debris deposits. Strike slip normal faults are formed on the left slope of the Hamam stream valley. On the basis of well logs and field observations, the slip distance in a unit time was calculated as a maximum of 100 m. There is another normal fault on the right slope of the valley. Since exposures are not continuous, faults cannot be traced well. However, the presence of thermal waters, sudden steep changes in topography and discontinuity in layers are the indicators of faulting. The youngest volcanic activity in the region started in the Miocene and continued until the Quaternary with some breaks. Acidic volcanism developed 10 km east and northeast of the spa, and the Elmadağ andesites located 15 km west of Banaz are the main volcanic units in the region. Quaternary Uşak-Kula volcanism (Ercan 1979). The footprints on volcanic ashes around the Salihli-Köprübaşı region are the most important evidence of recent volcanism. Kula Volcanites are products of deep tension cracks developed at the rigid continental crust at low temperatures and situated at a large distance from Büyük Menderes and Gediz Grabens (Öngür 2010a). The area shows evidence of several tectonic deformation phases in the bedrock.

In the study area fault systems of various directions are developed in association with the grabens of Western Anatolia. Normal faults observed in the study area are NE-SW (Ölmez 2000). In the study area and its surroundings, strike-slip faults and the developed extensional structures dependent on the grabens separate the strike-slip faults into segments, which form systems in opening fractures with high hydraulic permeability, and their end

Table 1 Results of chemical analyses and isotopic composition of the waters in the study area

Sampling point	Gazos sp.	Gazos sp.	Yayla mineral sp.	Hamamboğazi st.	Well-1	Well-2	Well-3,	Well-4	Sarikiz Sp.	Sarikiz sp.	F.Çuhadur water sp.
Sample no.	1	1	2	3	4	5	6	7	8	8	9
Date	27.07.2003	12.09.1950	27.07.2003	27.07.2003	27.07.2003	37,829	37,829	37,829	27.07.2003	12.09.1950	27.07.2003
Ca	133.8	364.2	108.6	80.20	90	113.4	114.8	125.4	113.4	347.9	121
Mg	192.5	125.7	243	81.2	182.4	243.2	237.5	194.2	200.9	115.2	101.2
Na	445	288.7	202	8.4	552	412	437	532	416	284.3	11.8
K	95	112.9	47	3.2	98	98	93	92	84	108.1	2.9
Cl	131	11.6	81.3	19.5	125.7	126	122	129	111.5	11.2	28.4
SO_4	624	1,111.3	142	118.5	670	604	896	635.6	634	1,081	221
HCO_3	1,691.5	1,106.9	1,839.1	494.1	1,745	1,828	1,506	1,887	1,596	1,155	586
SiO_2	84	40.3	11.8	18.8	86.8	77.7	83	87.5	74.5	74	15.1
B	12.8	n.m	5.6	0	13	12.2	12.4	12.2	12.5	n.m	0
F	8.9[a]	3.31	0.35	0	9.4[a]	2.73	3.31	2.82	3.18	n.m	0
As[a]	0.13	n.m.	0	0	2.44[a]	0.01	0	0	0.03	0.37	0
Fe[a]	0.12	0.09	0.02	0.04	0.28	0.28	0.06	0.01	0.52	0.12	0.03
Al	n.m.	2.29	1.14	<0.1	n.m.	n.m.	n.m.	n.m.	n.m.	2.28	<0.1
Li	2.1	n.m.	n.m.	<0.1	2.1[a]	2.0[a]	2.0[a]	2.1[a]	2.0[a]	n.m.	<0.1
T (°C)	42	–	18.1	15	64.5	65.5	72.5	72	54	–	16.4
pH (25°C)	6.5	6.7	6.3	7.5	6.9	6.9	7	6.9	6,8	6.9	7.1
EC (μS/cm)	4,410	n.m.	3,520	1,040	4,540	4,560	4,330	4,660	4,210	n.m	1,404
TDS (mg/l)	2,822.40	4,589.8	2,253	666	2,906	2,918.4	2,771	2,982	2,694	3,805	899
Total alk.	1,386.5	n.m.	1,507.7	405	1,430	1,498.5	1,234,5	1,547	13,008	1,308	480
CO_2	n.m.	1,210[a]	n.m	n.m	72.89[a]	n.m.	140[a]	389.5[a]	616	616	3.15[a]
$\delta^{18}O$ (‰SMOW)	−10.09	n.m.	−9.65	−9.18	−10.84	−11.16	−10.87	−10.95	−10.59	n.m.	−9.23
$\delta^{2}H$ (‰SMOW)	−77.12	n.m.	−69.65	−65.86	−74.99	−79.37	−73.21	−75.85	−75.89	n.m.	−63.8
^{3}H (TU)	00.00 ± 1.50	n.m.	8.35 ± 1.80	8.85 ± 1.80	0.00 ± 1.55	0.00 ± 1.65	0.00 ± 1.55	0.50 ± 1.80	2.70 ± 1.60	n.m.	6.40 ± 1.75
Water type	Na, Mg, HCO_3	Na, Mg, HCO_3	Mg, Na, HCO_3	Mg, Ca, HCO_3	Na, Mg, HCO_3	Na, Mg, HCO_3	Na, Mg, HCO_3	Na, Mg, HCO_3	Na, Mg, HCO_3	–	Ca, Mg, CO_3

Sample numbers correspond to the locality shown in Fig. 1. Cation and anion concentrations are in ppm

N.m. not measured, *TDS* total dissolved solids, *EC* electric conductivity

[a] Results taken from (Ölmez 2000)

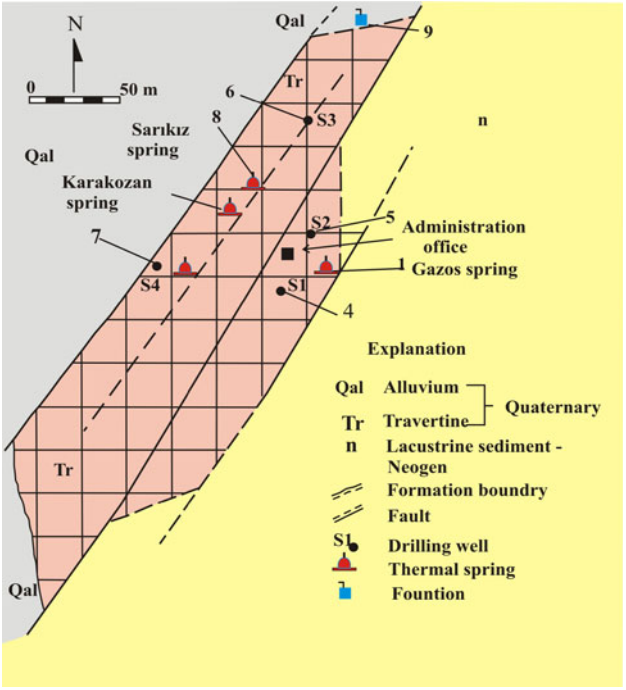

Fig. 2 Plan of water points in the study area

continues its effect into the very deepest points. In these types of areas where geothermal heat flows are not high, the existence of extremely high geothermal gradient formation can be explained by this tectonic formation (Ercan et al. 1997; Ölmez et al. 1998). In the geothermal wells drilled in the area, the geothermal gradient recorded is 65.7°C/1,000 m (Ölmez 1994).

The tectonic structures formed by the openings mentioned above reach various depths and provide conduits for groundwater to reach these depths, enabling circulation and heating. Generally, these types of waters filtered into the crust, forming the feeding water of geothermal fluid. The heat source of the geothermal system is related to these deepening young faults and Kula volcanics (Yilmazer et al. 2010).

Hydrogeology

Thermal and mineral waters of the Hamamboğazi spa are issued along the NE-SW trending normal faults. Faults behave as a conduit for the thermal waters. The temperature of the springs is between 30 and 54°C. Five wells were drilled by MTA and by ILB until late 2010 in order to determine the fluid potential of the area for the application of district heating in Banaz (Fig. 1). All the wells are of artesian type, and their depth is between 207 and 480 m. The water temperature ranges from 47.5–73°C. The total discharge is 325 l/s. As a result of the intense drilling, the discharge rates of the water decreased, and some of the springs dried up. In addition, well no. 1 was a flowing artesian well, and its pressure level was lowered when well no. 2 was drilled (Ölmez 1994). Travertine deposits precipitating from thermal waters that flow out from the fault structures around the spas cover an area of $\sim 50\ m^2$, especially along the fault line where the Hamamboğazi springs discharge. They have a thickness of about 75–80 m. Their formation still continues. Gas also emanates from near the top of the deposit. Travertine deposition blocks out fluid paths, causing the springs to migrate over time.

Schists in the Paleozoic series that are exposed around the Banaz Hamamboğazi spa are mostly impermeable. Due to their secondary porosity and permeability, ophiolitic rocks, fractures and cracks in alternating marble and limestone are thought to be the primary aquifers for thermal and cold waters (Pasvanoğlu et al. 2005). The permeability of the lacustrine deposits of 250–400 m thickness formed by clayey layers is relatively low. Therefore, lacustrine deposits are the cap rocks of the reservoir. Cold waters penetrating through the fractures and cracks in the granite intrusion (Süer et al. 2010) of the Murat Mountains in the north and Catmali Mountain in the south comprise the recharge area (Pasvanoğlu et al. 2005). These waters, which are heated at depth, fill the fractures, cracks and karstic voids of the marbles and, rising along the permeable zones, form the thermal waters of Banaz (Hamaboğazi) spa. The temperature of the springs is between 30 and 54°C, while the temperature of the artesian water of well no. 3 is up to 73°C (at 293 m depth).

Water chemistry

The pH values for thermal waters are between 6.5 and 7.1, but for cold water springs are between 7.1 and 7.5. The TDS (total dissolved solids) content of thermal waters ranges from 2,982 to 2,694 mg/l, but for cold waters is between 666 and 899 mg/l. Electrical conductivities range from 4,210 to 4,660 μmho/cm for thermal waters and 1,040 to 1,404 μmho/cm for cold water. Banaz mineral water attains a maximum pH, TDS and EC values of 6.3, 2,253 mg/l and 3,520 μS/cm, respectively (Table 1).

Compositions of thermal and cold waters collected from the study area were compared in a Schoeller (1962) diagram (Fig. 3). In a semi-logarithmic diagram of the thermal and mineral waters, the lines connecting the milli-equivalent values of ions are almost parallel, indicating that the waters are of similar origin. According to the Association of International Hydrogeologists (IAH 1979), the Banaz waters are Na, HCO_3, SO_4, B, SiO_2, F, As, and CO_2 type. Degassing of CO_2 gas in springs facilitates travertine

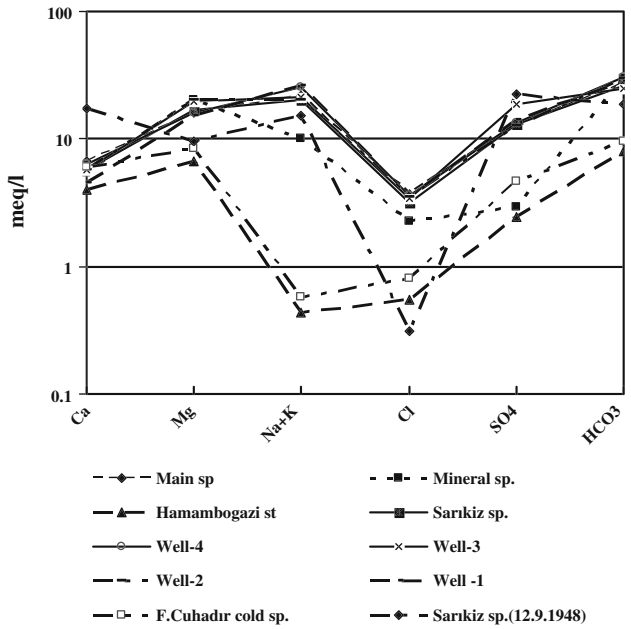

Fig. 3 Schoeller diagram. Numbers are the same as in Table 1

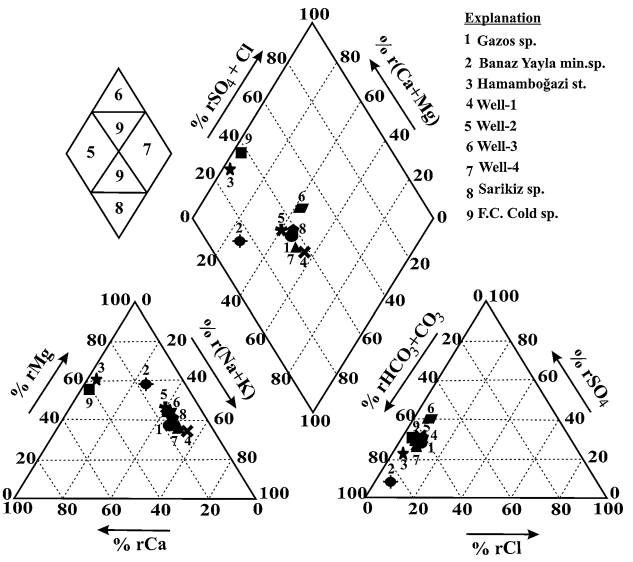

Fig. 4 Piper diagram

deposition. Water-rock interaction is related to the thermodynamic disequilibrium of minerals under varying pressure and temperature conditions in a fluid phase comprised by water and gas (Stumm and Morgan 1965). There was a significant change in the composition of Sarikiz spring in 1948 (Çağlar 1950) and 2003. Ca^{+2}, K^{+} and SO_4^{-2} concentrations of the water in 2003 decreased, whereas Mg^{+2}, Na^{+}, Cl^{-} and HCO_3^{-2} concentrations significantly increased. Banaz thermal and mineralized waters are bicarbonate-rich waters. They have 52.77–65.01% of the total miliequivalent values of cations. Due to their higher temperatures and thus increasing solubility, thermal waters have a high Na^{+} and K^{+} content.

Na^{+} in waters is derived from dissolution of Na-bearing salts or alteration of feldspars in ultrabasic rocks and schists. Clay minerals also enhance the exchange of Na^{+} with Ca^{+2}. It is comprised of 38.63–51.93% of the total milliequivalent values of cations. The concetration of Ca^{+2} (9.79–15%) and Mg^{+2} (32.89–43.72%) is lower than Na^{+}. Low Cl^{-} concentration in this type of waters is attributed to mixing of ascending thermal waters with cold groundwater. Decreasing Cl^{-} and increasing HCO_3^{-2} concentrations in thermal waters may indicate increasing water-rock interaction (Giggenbach and Glover 1992). The presence of Cl^{-} up to 7.35–8.31% indicates that some of the ions in these waters are derived from volcanic activity. The source of SO_4^{-2} is explained by the oxidation of H_2S and/or dissolution of minerals like gypsum within the Neogene sediment. High bicarbonate concentrations are due to the reaction of CO_2-rich waters and limestone and marbles during the circulation of meteoric waters. Calcite is the main material they precipitate (Browne 1991).

A Piper (1944) diagram indicates that thermal waters of Banaz are Mg–Na–HCO_3 water (Fig. 4). Na–HCO_3 waters are common in geothermal systems associated with metamophic rocks, which is consistent with the general lithology of the Menderes Massif. The origin of the high dissolved CO_2 according to $\delta^{13}C$ and He isotopic data is magmatic (Ercan et al. 1990; Vural et al. 2008; Filiz 1982). The Na–HCO_3 chemical composition is therefore a combination of high CO_2 flux and extensive water-rock interactions with metamorphic rocks (Vengosh et al. 2002). Cold waters with carbonate hardness of more than 50% plot into field no. 5, which indicates calcite dissolution. These waters are of Ca–HCO_3 and Mg–CO_3 type and represent shallow circulating ground waters with low TDS and EC.

All thermal waters in the area contain more than 12 mg/l of boron. High boron content is attributed to deep water circulation. Its source could be the Neogene volcanism or serpentines. The silica concentration in the waters is between 74.5 and 87.5 mg/l. Most of silica is derived from the alteration of silicate minerals in chert, magmatic and metamorphic. As most of the Fe^{+2} in spring waters rapidly precipiates once it comes in contact with air, the amount of Fe^{+2} in waters is between 0.01 and 0.52 mg/l. Red-brown-colored iron oxide precipitates are common in areas where springs are manifested. Moreover, travertines of the same color are also observed. Iron most probably was transferred to the water by oxidation of hematite and pyrite in volcanic rocks (Şahinci 1991).

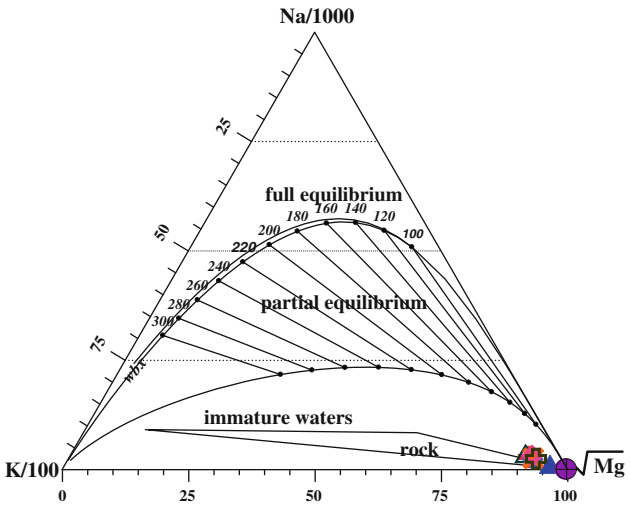

Fig. 5 Plot of Na–K–Mg equilibrium diagram. Numbers are the same as in Table 1

$$4FeS_2 + 15O_2 + 10H_2O \rightarrow 4HFeO_2 + 16H + 8SO_4 \quad (1)$$

CO_2 gas is detected in all the thermal waters (Table 1). CO_2 emanations are also measured from fractures and fissures in several parts of the field. The amount of CO_2 in water is between 72.89 and 1,210 mg/l. Some carbon dioxide may be derived from volcanism, while some is the product of chemical reactions between carbonate and acids.

Concentrations of the elements As and Li are relatively quite high in Hamamboğazi. Li increases in relation to the time of the interaction with clay. The increase of As concentration is related to the interaction between the hydrothermal decomposition zone and water. The Banaz Hamamboğazı thermal waters are characterized by the high F content (2.73–9.4 mg/l, Table 1) compared to that reported for other thermal waters in the western Anatolia region and shows temporal variation. These thermal waters are being used in spas at present. Considering the As and fluoride contents, which are much higher than the prescribed limit for drinking water standards of 10 ppb (As) and 1.5 ppm (F) by the WHO (2003), caution should be exercised when using cold spring water for drinking purposes. As shown in Table 1 and Fig. 5, mixing of thermal water and cold spring water is taking place at the near surface environment, and thus contamination of groundwater used for domestic purposes is possible.

The AquaChem computer program, Calmbach (1997), was used to compute the saturation index of various carbonate, sulfate, silica and silicate minerals at the outlet temperatures of the waters. The results show that the thermal waters of Banaz Hamamboğazi are oversaturated with respect to calcite, aragonite, dolomite, chalcedony, quartz, K-feldspar, K-mica, Ca-monmorlinite and kaolinite. Although most samples are sulfate-enriched, none of them are oversaturated or in equilibrium with anhydrite, gypsum and fluorite. This may imply that the SO_4 concentration of the waters is controlled by a steady-state dissolution process (Grasby et al. 2000). Cold waters are oversaturated with respect to calcite, dolomite, aragonite and quartz, and undersaturated with other minerals.

Geothermometers

To determine reservoir temperatures of the Banaz Hamamboğazi geothermal waters, various silica and cation geothermometers were used (Table 2). Different reservoir temperatures calculated for the Banaz waters indicate that concentrations of silica and cations in these waters are affected by some chemical processes such as mixing and evaporation, as well as by the use of different constants in geothermometers proposed by various authors. Of the silica geothermometers, the quartz and chalcedony geothermometers yield reservoir temperatures of 111–130°C and 93–103°C, respectively. As stated by Fournier (1991), the solubility of silica at temperatures less than 180°C is controlled by chalcedony rather than quartz, and by both minerals in some cases. The SiO_2 content of fluids is relatively low, suggesting that thermal waters rise to the surface without equilibration because of their rapid circulation. These waters may also precipitate silica or mix with dilute cold waters that return to the surface. Thus, the tempratures calculated using silica geothermometry (93–130°C, Table 2) can be considered as the minimum temperature of the thermal reservoir. However, the temperatures calculated from cation geothermometers vary widely and give reservoir temperatures higher than the silica geothermometer. The Na–K geothermometers of Fournier (1979) and Giggenbach (1988) give temperature ranges of 269–305°C and 280–313°C, respectively. It is obvious that Na–K geothermometers applied to the Banaz geothermal field give anomalously high temperatures and suggest a deeper reservoir.

In order to eliminate the possible effects of Ca concentrations on the Na–K geothermometer, the Na–K–Ca geothermometer of Fournier and Truesdell (1973) was used. The reservoir temperatures calculated from this geothermometer yield a maximum temperature of 227°, which is lower than that of the Na–K geothermometers, but still higher than those of the quartz and chalcedony geothermometers.

Based on Fig. 5 proposed by Giggenbach (1988), all the data points plot in the area of immature waters; therefore, solute geothermometry is not likely to yield meaningful equilibration temperatures. The presence of travertine associated with spring shows that the discharge

Table 2 Geothermometer results for Hamamboğazi thermal waters (°C)

Geothermometer (°C)	Gazos sp.	Well 1	Well 2	Well 3	Well 4	Sarikiz sp.
$T\ ^{\circ}C_{measured}$	63	64.5	73	70	62	54
$Quartz^{a}_{no\ st.loss}$	128	130	124	127	130	122
$Quartz^{a}_{max.st.loss}$	125	126	121	124	127	120
$Quartz^{b}_{no\ st.loss}$	119	120	114	117	121	111
$Quartz^{b}_{max.st.loss}$	124	125	120	123	126	118
$Chalcedony^{a}_{no\ steam\ loss}$	100	102	96	99	103	93
$Chalcedony^{a}_{max.st.loss}$	100	102	96	100	102	94
$Chalcedony^{b}_{no\ st.\ loss}$	99	101	95	99	101	93
$Chalcedony^{b}_{max.st.loss}$	100	102	97	100	102	95
Na/K^{c}	292	272	305	292	269	286
Na/K^{d}	301	283	313	301	280	296
$K–Mg^{d}$	62	63	61	61	62	60
$Na–K–Ca^{e}$	226	223	234	228	217	223

Sample numbers and names are the same as in Table 1

[a] Fournier (1973)

[b] Arnorsson et al. (1983)

[c] Fournier (1979)

[d] Giggenbach (1988)

[e] Fournier and Truesdell (1973)

temperatures and probably the temperatures at depth were appreciably hotter in the distant past.

The thermal water of Banaz reacted with sedimentary formations and mixed with cold springs at the near surface enviroment, thus losing its true chemical composition. The sediment, thermal water and cold water interaction is seen in the reservoir temperatures estimated using a K–Mg geothermometer (Table 2) where the obtained values are lower than the temperatures measured at the surface and at the bottom of wells. Thus, on Giggenbach's (1988) Na–K–Mg diagram, all the thermal spring waters move away from the equilibrium/partial equilibrium field and plot near the Mg corner. Therefore, the usefulness of the application of both K–Na and K–Mg, and indeed any type of cation geothermometer, is doubtful, and the interpretation of the temperature predictions of such waters should be made cautiously (Giggenbach 1988).

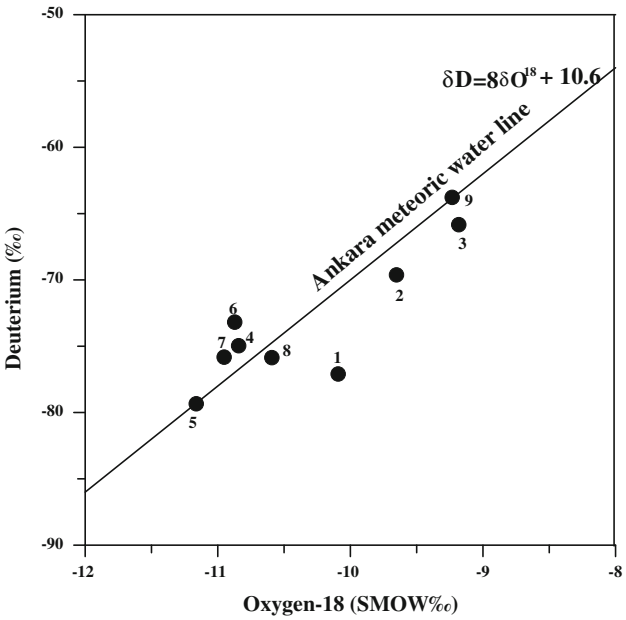

Fig. 6 $\delta^{18}O$–Deuterium diagram. Numbers are the same as in Table 1

Evaluation of isotopic data

In this section, based on (^{18}O), (^{2}H) and (^{3}H) contents of waters from springs and wells in the Banaz area, the circulation system of the groundwater, recharge-discharge and hydrogeologic characteristics of aquifers are investigated. Using the stable isotope data, the $\delta^{18}O$–$\delta^{2}H$ graphic was drawn (Fig. 6). The meteoric water line equation of the Ankara region ($\delta^{2}H = 8\delta^{18}O + 10.6$) proposed by DSI (Mesut Sayın (2009) personal commuication) was taken for the study area. Samples are plotted very close to this line, indicating that they are of meteoric origin (Pasvanoğlu 2007). These waters percolate downwards through faults and fractures, and are heated by a geothermal gradient, then rise to the surface along permeable zones. The isotopic compositions of Banaz thermal waters are more negative in comparison to those of cold waters, which may indicate

that thermal waters are recharged by continental precipitation in elevated areas. Since isotopic compositions of Banaz Yayla mineralized water and F.C. cold water are plotted at the right side of the meteoric line, waters recharging these springs may have been subjected to an evaporation process. This is also supported by the fact that impermeable rocks in the area are widely exposed at lower elevations. In addition, under very hot conditions, evaporation is expected to occur before the filtrations. Moreover, this may also occur as a result of oxygen exchange between CO_2 and thermal waters, yielding more negative oxygen-18 values (Clark I and Fritz 1997). However, Banaz thermal waters with similar values are deeply circulated waters that are recharged from higher elevations in the Murat Mountains in the north and Catmali Mountain in the south. It is noticeable that thermal waters, particularly in Gazoz thermal spring (no. 1), are represented by more negative oxygen-18 values and significantly shift from the meteoric line, which has resulted in an increase of the $\delta^{18}O$ content of these waters. Such a shift in $\delta^{18}O$ occurs because of the exchange of oxygen isotopes between water and rock. This is confirmed by the relatively high TDS contents and temperatures of these waters. Enrichments of ^{18}O and deuterium may indicate that thermal waters are recharged from a different source, probably from a higher elevation (1,500–2,300 m).

The Banaz Yayla mineralized water (no. 2) and the Hamamboğazi stream water (no. 3) are characterized by a tritium content of 8.35 and 8.85 TU, respectively (Fig. 7). These waters are shallowly circulated and fed by low-altitude recent precipitation, and they have a short residence time. Relatively high TDS content coupled with EC, Cl and isotope data on these waters could indicate that they may mix with thermal waters of deep origin. F. Cuhadur cold (no. 9) spring waters are recharged by inland precipitation from high elevations and characterized by residence times shorter than that of thermal waters. The tritium content of the thermal waters is below 1 TU, indicating a very deep circulation and long residence time, except for Sarikiz spring (no. 8). Deuterium depletion and the very different tritium content (2.7 TU) of the Sarikiz spring (no. 8) water can be described by mixing of this water with surface waters.

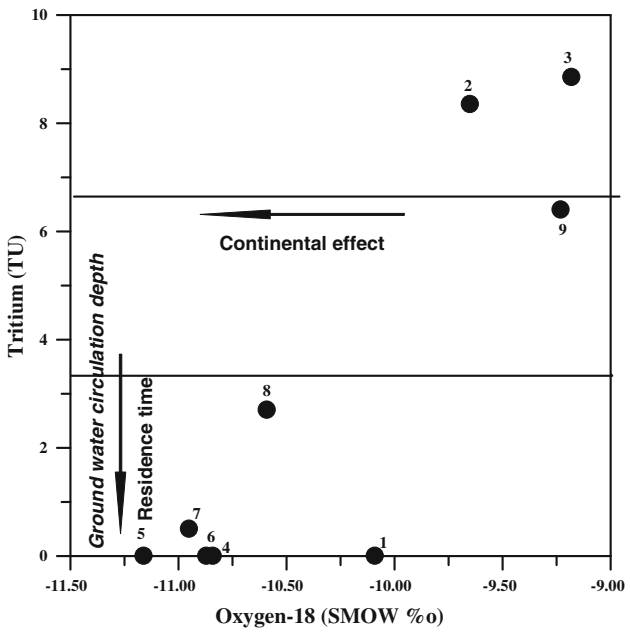

Fig. 7 $\delta^{18}O$–Tritium diagram. Numbers are the same as in Table 1

Evaluation of the geothermal system in the study area

The Banaz-Hamamboğazi geothermal field is a liquid-dominated system with a reservoir temperature of about 100°C (from geothermometry). A volumetric method is used to calculate the potential of the geothermal prospect following Hochstein (1975). The volumetric method involves the calculation of geothermal energy contained in a given volume of rock and water, but neglects all recharge to the system. The results obtained by this method are convenient for rough estimates of the resources (Saptadji 1987). The thermal energy in the subsurface is calculated as follows:

$$E = E_r + E_w = VC_r\rho_r(1-\Phi)(T_i - T_o) + VC_w\rho_w\Phi(T_i - T_o) \quad (2)$$

where E = total energy in the rock and water (kJ); V = reservoir volume (m^3); T_i = temperature of the aquifer (°C); T_o = reference temperature (°C); C_r = specific heat capacity of rock (kJ/kg°C); C_w = specific heat capacity of water (kJ/kg°C); ρ_r = density of reservoir rocks (kg/m^3); ρ_w = density of water (kg/m^3); Φ = porosity; hf = enthalpy.

For the Banaz geothermal field the following assumptions were made:

$A = 1\ km^2$; $V = 5 \times 10^8\ m^3$; $T_i = 73°C$ (high temperature measured in well no. 3 as 73°C); $T_o = 15°C$; $\rho r = 2{,}641\ kg/m^3$ (Goodmans 1989); $\rho_{w73°C} = 976.01\ kg/m^3$; $hf_{73°C} = 305.6$ kJ/kg; $hf_{30°C} = 125.7$ kJ/kg (Zarrouk and Watson 2001); $\Phi = 0.06$; $C_r = 0.804$ kJ/kg°C; $C_w = 1$ kJ/kg°C (at 73°C all the water is liquid); $\Delta T/\Delta Z = 30°C/km$; thickness = 500 m; hence, the normal temperature gradient is $30 \times 500/1{,}000 = 15°C$). The difference between temperatures is $\Delta T = (73-30)$.

Using the above-stated parameters in the equation, the total heat energy in a volume (V) of fractured reservoir beneath a specified area that can be used by space-heating is 5.086E 16 J.

The power potential can be calculated by using the recovery method (Hochstein 1975). An arbitrary recovery factor of $r = 0.25$ can be assumed. There is no theoretical justification for using this value, except that it provides a rough magnitude that often is of the "right order." The value of "r" is actually controlled by the efficiency of naturally induced recharge, permeability structure of the the reservoir and fluid characteristics.

Using stored heat and the recovery method, we assume a recovery factor of 0.25 and lifetime for exploration of 25 years; assuming also that the geothermal system works 365 days per year, the power potential estimated for the Banaz geothermal field is 16 MW_t.

Conclusion

A geological map (1:25,000) of the 16 km^2 area around the spa was made, and characteristics of thermal and cold waters were determined. Thermal waters of the Hamamboğazı spa are manifested through NE-SW-trending normal faults. Based on the present study, a hypothetical model for the evolution of the Banaz thermal waters was developed and is shown in Fig. 8. The thermal waters have a temperature of 30–54°C. Ophiolitic rocks, Paleozoic schist, marbles and limestones below the lacustrine units arround the spa are believed to be possible reservoir rocks because of their extremely fractured character. The heat source of all geothermal systems in Gediz Graben is probably related to the Kula volcanism. In addition, tectonic activities in association with volcanism transfer the magma heat to the surface, and therefore, the geothermal gradient in these fields is high. Cold waters penetrating through the fractures and cracks in the granite intrusion of the Murat Mountains in the north and Catmali Mountain in the the south comprise the recharge area. These waters, which are heated at depth, fill the fractures, cracks and karstic voids of marbles and, rising along the permeable zones, form the thermal waters of Banaz Hamamboğazi spa.

Cold waters are of Ca–Mg–HCO_3 type and represent shallow circulating ground waters with low TDS and EC. The Banaz geothermal field is a liquid-dominated system with estimated reservoir temperatures ranging from 93 to 130°C. These waters are made up of Na–HCO_3 of meteoric origin. They are deep, circulating recharge waters from higher enhanced elevations. The thermal waters contain tritium (0 to $\sim$3 TU). The tritium could be from mixing, or it could indicate rapid circulation with too little time for the tritium to decay.

The high concentrations of B, F and As in Banaz thermal water cause F and As contamination of cold groundwaters used in the area. Caution should be exercised when using cold spring water for drinking purposes.

On the basis of mineral equilibrium calculations performed at the discharge temperatures of the thermal waters, carbonate and silica minerals show equilbrium saturation. Although most of the samples are sulfate enriched, all waters are undersaturated with respect to gypsum and anhydrite, and this may indicate that the SO_4 concentration of the waters is controlled by a steady-state dissolution process. Due to carbonate oversaturation, scaling problems are expected during production.

The potential of the geothermal area investigated is found to be suitable for heating of Banaz. On the basis of

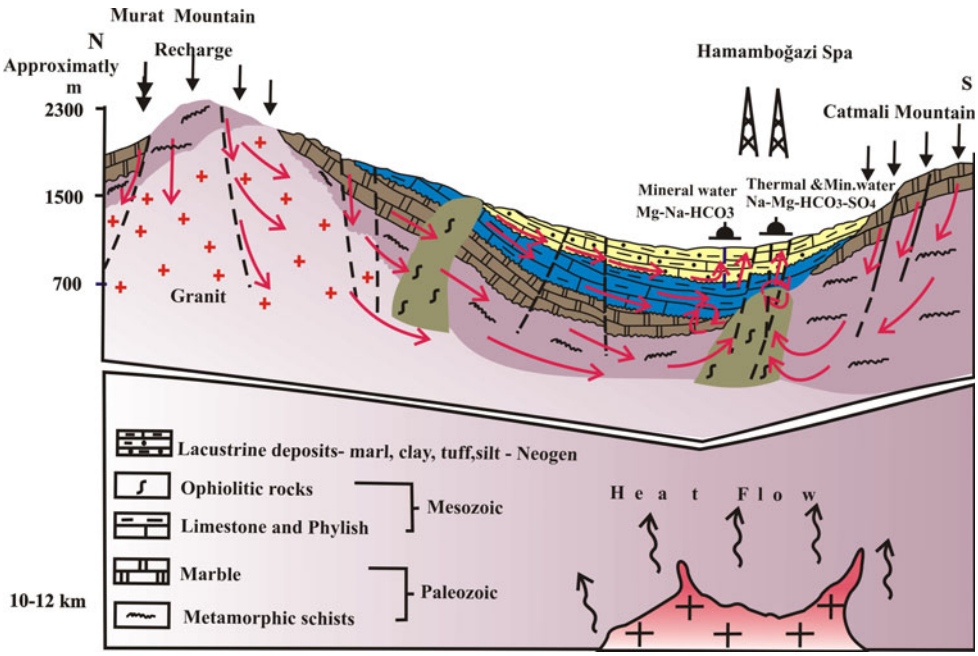

Fig. 8 A general hydrological model of the Banaz Hamamboğazi area

their isotope compositions, thermal waters of meteoric origin are deeply circulated waters characterized by long residence times and recharged by rainwater of high elevations. The usable total energy potential of the Banaz field is about 5.086E 16 J. Its estimated power potential is 16 MW_t.

The present study supports the existence of a high-temperature reservoir below Banaz Hamamboğazi geothermal province. The geothermal potential of the study area has not been assessed up to now. Hydrothermal fluids to be produced with suitable methods could be used for central heating, tourism and greenhouses sectors. Moreover, since Banaz is located at the center of Izmir, Ankara, Eskişehir and Denizli cities, and it is surrounded with forests, plateaus and mountains, it is clear that thermal tourism in the area will develop rapidly if the necessary investments are made. The Banaz Yayla mineralized water (no. 2) is very tasty. Its chemical composition is composed of Mg, Na, HCO_3 and CO_2. Once necessary facilities are established, this mineral water should be bottled immediately. This attempt will promote evaluations of other mineral waters around the Banaz area. Development and expansion of the thermal water facilities in the Banaz area are no doubt dependent on drilling of deep wells and thus increasing hot water discharges. There is such a potential in the study area, and proposed projects and investments should be started at once.

Acknowledgments I extend my special appreciation to Dr. Zbigniew Malolepszy for the English editing of this article. I also thank the editorial team of Environmental Earth Science for their critical review and comments of an earlier version of this manuscript.

References

APHA (1989) American Public Health Association (APHA), American Water Work Association (AWWA), Water Pollution Control Federation (WPCF). Standard method for the determination of water and waste water, 5th edn publishing, Washington DC

Arnõrsson S, Gunnlaugsson E, Svavarsson HI (1983) The chemistry of geothermal waters in Iceland. III. Chemical geothermometry investigations. Geochim Cosmochim Acta 47:567–577

Browne PRL (1991) Minerological guides to interpreting the shallow paleohydrology of epithermal mineral depositing environments. Proc 13th NZ Geothermal work-shop, Auckland, pp 263–270

Çağlar KÖ (1950) Türkiye maden suları ve kaplıcaları MTA yayını seri B No:11 Fas 3, Ankara pp 454–456

Calmbach L (1997) AquaChem computer code-version 3.7.42, waterloo hydrgeologic. Waterloo, Ontario N2L 3L3.

Canik B, Başkan EM (1983) IAH Map of mineraland thermal waters of Turkey Aeagean region, MTA Publ No 189

Clark ID, Fritz P (1997) Environmental isotopes in hydrogeology. Lewis Publ, Boca Raton

Ercan T (1979) Cenozoic volkanizm in western Anatolia, Thrace and the Aegean Islands. Jeoloji müh. Sayı 9, Ankara, pp 23–46

Ercan T (1982) Batı Anadolu'nun genç tektoniği ve volkanizması paneli. Ankara, pp 5–14

Ercan T, Matsuda JI, Nagao K, Kita I (1990) Anadoludaki sıcak sularda bulunan doğal gazların izotopik bileşimleri ve karbondioksit gazının enerji açısından önemi

Ercan T, Satır M, Sevin D, Türkecan A (1997) Batı anadolu'daki tersiyer ve kuvaterner yaşlı volkanik kayaçlarda yeni yapılan radyometric yaş ölçümlerinin yorumu. MTA Dergisi 119:103–112

Filiz Ş (1982) Ege bölgesindeki önemli jeotermal alanların ^{18}O, ^{2}H, ^{3}H, ^{13}C izotoplarıyla incelenmesi. Doçentlik Tezi, E.Ü. Y.B.F. (Unpublished)

Fournier RO (1973) Silica in thermal waters: laboratory and field investigations. In: Proceedings of international symposium on hydrogeochemistry and biogeochemistry, Tokyo, pp 132–139

Fournier RO (1979) A revised equation for the Na–K geothermometer. Geothermal Res. Council Trans vol 3. pp 221–224

Fournier RO (1991) Water geothermometers applied to geothermal energy. In: D'Amore F Applications of geochemistry in geothermal reservoir development. UNITAR/UNDP publication, Rome, pp 37–69

Fournier RO, Truesdell AH (1973) An empirical Na–K–Ca geothermometer for natural waters. Geochim Cosmochim Acta 37:1255–1275

Giggenbach WF (1988) Geothermal solute equilibrium. Derivationof Na-K-Mg-Ca geoindicators. Geochim Cosmochim Acta 52: 2749–765. NITAR/UNDP Publication Rome, 119–142

Giggenbach WF, Glover R (1992) Tectonic regime and major processes govering the chemistry of water and gas discharges from the Rotorua geothermal field? Geothermics, 21(No ½):121–140

Goodmans R (1989) Rock mechanics, 2nd edn. Wiley Sons, NY

Grasby SH, Hutcheon I, Krouse HR (2000) The influence of water-rock interaction on the chemistry of thermal springs in western Canada. Appl Geochem 15:439–454

Hochstein MP (1975) Geophysical exploration of the Kawah Kamojang geothermal field, W. Java. Proc. 2nd UN symposium on development of geothermal resources, pp 1049–1058

IAH (International Association of Hydrogelogists) (1979) Map of mineral and thermal water of Euarope. Scale 1:500,000. International Association of Hydrogelogists United Kingdom

Ölmez E (1994) Uşak Banaz Hamamboğazi–2 (HB–2) sıcak su sondajı, MTA Rap No: 9804, Ankara

Ölmez E (2000) Uşak-Banaz Hamamboğazı jeotermal sahası jeolojihidrojeoloji etüdü MTA Rap, Ankara

Ölmez E, Ercan T, Yilmazer S (1998) Batı Anadoluda yüksek tuzlulukdaki jeotermal sistemler. 75 Yıl Semposyumu bildirileri, Ankara

Öngür T (2010a) Geologic and thermal evolution of Turkeys wealthy geothermal region MMM. In: Proceedings World Geothermal Congress (WGC 2010) 25–29 April, Bali

Öngür T (2010b) Derinden Jeotermal dünyası 4. Jeotermal dünyasına ilişkin haberler yazılar kişisel görüşler

Pasvanoğlu S (2007) Geothermal energy possibilities of the Banaz Hamamboğazi area, Turkey. In: 12th International Symposium on water-rock interaction July 31–August 5, China

Pasvanoğlu S, Canik B, Arigün Z (2005) Geothermal Potential of the Banaz Hamamboğazi thermal and mineralized waters. In: Proceedings World Geothermal Congress (WGC 2005) 24–29 April, Antalaya

Piper AM (1944) A graphic procedure in geochemical interpretation of water analyses. Am Geophys Union Trans 25:914–923

Şahinci A (1991) Doğal suların jeokimyası reform matbaası Izmir

Saptadji NM (1987) Reservoir simulation of kamojang field. Geothermal Institute Project report 87 School of Engineering library. University of Auckland, New Zealand

Schoeller H (1962) Les eaus souterrians Masson et. Cie, Paris

Şimşek Ş (1997) Geochemical potential in Northwestern Turkey. In: Schindler C, Pfister M (eds) Activetectonics of Northwestern Anatolia—The Marmara Poly-Project Zürich, pp 111–123

Stumm W, Morgan JJ (1965) Aquatic chemistry–an intruduction emphasizing chemical equilibria in natural waters, 2nd edn. Wiley Interscience, NY

Süer S, Wiersberg T, Güleç N, Erzinger J, Parlaktuna M (2010) Geochemical Monitoring of the Seismic activities and noble gas characterization of the geothermal fields along the eastern segment of the Büyük Menderes Graben. In: Proceedings World Geothermal Congress (WGC2010) 25–29 April, Bali

Vengosh A, Helvacı C, Karamanderesi IH (2002) Geochemical constraints for the origin of thermal waters from western Turkey. Appl Geochem 17:163–183

Vural S, Pasvanoğlu S, Yilmazer S, Yakabağ A (2008) Urganli (Turgutlu) Sıcak ve Mineralli Sularının Izotoplarla Incelemesi. III. Ulusal Hidrolojide Izotop Teknikleri Sempozyumu, D.S.I., Istanbul, pp 255–271

WHO (2003) Guidelines for drinking water quality, 3rd edn. Radiological Quality of Drinking Water, World Health Organization, Genova

Yilmazer S, Pasvanoğlu S, Vural S (2010) The relation of geothermal resources with young tectonics in the Gediz graben (West Anatolia, Turkey) and their hydrogeochemical analyses. In: Proceedings World Geothermal Congress (WGC 2010) 25–29 April, Bali

Zarrouk SJ, Watson A (2001) Thermodynamic and transport properties of saturated steam and water. University of Auckland, New Zealand